RPE | Radiation Physics & Engineering
A Peer-Reviewed Journal
Published by K.N. Toosi University of Technology
http://rpe.kntu.ac.ir
Research Article

Radiation Physics and Engineering 2023; 4(1):39–51

Isotopic discharge concentrations of Tehran research reactor using deterministic and Monte Carlo methods

Farrokh Khoshahval*, Mohammad Rajaee, Nafiseh Tehrani

Reactor and Nuclear Safety Research School, Nuclear Science and Technology Research Institute (NSTRI), Tehran, Iran

HIGHLIGHTS

- Fuel isotope inventories were calculated for the first and 83rd core configuration of the Tehran Research Reactor.
- It is shown that the 94% of the TRU produced during the TRR operation is Pu.
- The total radioactivity of the TRR core at the end of the reactor core life (Core83) is estimated to be 6.47×10^5 Ci.

ABSTRACT

Actinide concentration and activity analysis of the nuclides resulted from the burnup (depletion) process during nuclear reactor operation lifetime is an essential problem in reactor design. Inventory and the corresponding activities of the Tehran Research Reactor (TRR) are evaluated using different methods and compared with each other. WIMS-CITATION, ORIGEN, and MCNP codes are used for plate type inventory calculations. The important actinides, fission products, and fissile inventory ratio of TRR have been calculated at different burnup steps. It is worth noting to mention that knowing the value of inventory helps us for safe handling of the spent fuels and to have a perfect design for transport cask of spent fuels. In this work, the fuel isotope inventories were calculated for the first and 83rd core configuration of the Tehran Research Reactor, which is named "Core01" and "Core83" respectively. The calculations were first performed using WIMS-D5 and CITATION neutronic codes and then the results are compared with that of ORIGEN and MCNPX code. The total radioactivity of the TRR core at the end of the reactor core life (Core83) is estimated to be 6.47×10^5 Ci.

KEYWORDS

TRR reactor
Inventory
Activity
Actinide
Concentration

HISTORY

Received: 16 June 2022
Revised: 3 August 2022
Accepted: 6 August 2022
Published: Winter 2023

Nomenclature

Burn up (%)	The percentage of loss of the number of U-235 Atoms
CFE	Control Fuel Element
CZP	Cold Zero Power
GR-BOX	Graphite Box
FPD	Full Power Day
HFP	Hot Full Power
HFX	Hot Full Power, Xe equilibrium
HZP	Hot Zero Power
IR-BOX	Irradiation Box
SFE	Standard Fuel Element
TRR	Tehran Research Reactor

1 Introduction

The prediction of the properties change during nuclear reactor operation lifetime is one of the most critical problems in reactor design. Knowing the behavior of the reactor throughout its life ensures that the reactor core will operate safely. It also helps to determine the time that the reactor will remain critical at the desired power level. Furthermore, it is important from the viewpoint of waste management (for instance, the disposal of the minor actinides), fuel storage, and transportation and reprocessing. So the fuel isotopes inventory evaluations and the calculation of the residual fission products and their toxicity would be interesting (IAEA, 1992). It is also important for decay heat modeling and behavior of fuel during irradiation due to the produced fission products (Al Zain et al., 2018). Also, good knowledge of the inventory is necessary for the disposal of the spent fuels in an environmentally safe manner. Because of geometry, data complexity, and cumbersome equation governing the nuclear reactor behavior, selecting the best model or code to reach the best result has great importance. In other

*Corresponding author: f_khoshahval@sbu.ac.ir

https://doi.org/10.22034/rpe.2022.347567.1092
https://dorl.net/dor/20.1001.1.26456397.2023.4.1.6.0

words, in the nuclear reactor calculations, the accuracy of the computed value and the computation time are the two most important parameters. Numerous investigations have been conducted regarding inventory calculations. For instance, Ref. (Khattab, 2005) calculated the inventory of some important radionuclides in the Miniature Neutron Source Reactor using WIMS4D code. In another study, the MTRPC package is applied for burnup calculation of Miniature Neutron Source Reactor, MNSR (Hassan et al., 2008). It is found Sm-149 followed by Gd-157 play an essential rule in lifetime of MNSRs.

The primary purpose of the present investigation is to evaluate WIMS-CITATION and ORIGEN codes for inventory and activity calculation for MTR plate-type Tehran Research Reactor (TRR). TRR is the only pool-type research reactor under operation in Iran. During reactor operating lifetime, the isotopic composition changes in the macroscopic cross-section which can be calculated using the transport code. In this study, WIMSD-5 was employed to calculate the cross-sections in each burnup step (Halsall, 1982). In this paper, the inventory calculation of the TRR is computed using a developed Fortran 90 language programming which has coupled WIMS and CITATION LDI-2 codes (Fowler et al., 1999). The obtained results using WIMS-CITATION have been compared with one-dimensional ORIGEN2 code (Croff, 1980a) at different burnup steps. In some cases, the results are also compared with the Monte Carlo code, MCNPX.

2 Tehran Research Reactor characteristics

Tehran Research Reactor is a 5 MW reactor using U3O8-Al MTR type fuel (IAEA, 2009). The SFE and CFE are made of 19 and 14 fuel plates, respectively. The main design data are given in Table 1 (IAEA, 2009). The necessary components of TRR are SFE, CFE as fuels, IR-BOX, GR-BOX, and Grid-Plate which are demonstrated in Figs. 1 and 2. The first core configuration with fresh fuels is shown in Fig. 3. It is worth mentioning that the exit burnup that is considered for the fuel assembly of TRR is around 45% to 60% (it depends on the operational conditions). But the cycle length of TRR is about 20 to 35 FPD. The point is that after each cycle, the burnup of each fuel assembly increases about 2%. At the end of each operating cycle, only one fuel assembly with the highest burnup would be exited from the core and one fresh fuel assembly would be added to the TRR. Indeed, the fuel management of research reactors is usually very different from that of power reactors.

3 Calculation Methodology

There are several computer codes available to evaluate nuclide production and depletion. Among them, WIMS-CITATION, ORIGEN, and MCNPX are the most well known codes. This paper calculates the concentrations of the most important generated isotopes during reactor operation and compares the results of the mentioned codes.

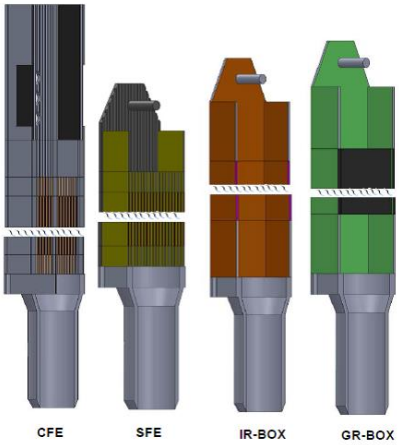

Figure 1: The main components of the TRR reactor which are placed in grid plate.

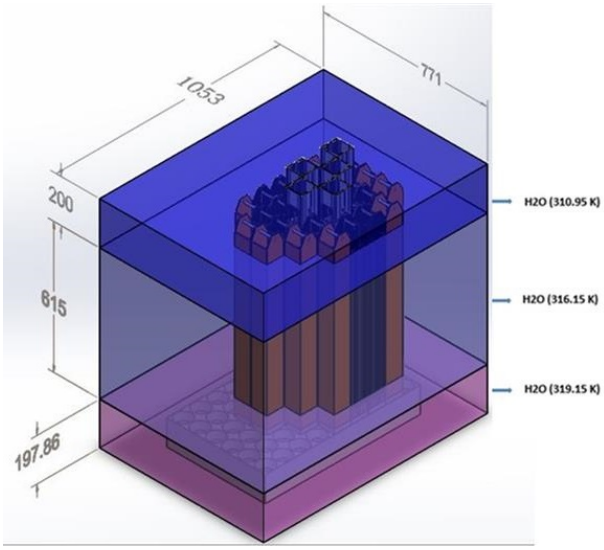

Figure 2: Cross-sectional view through Tehran Research Reactor, "Core01".

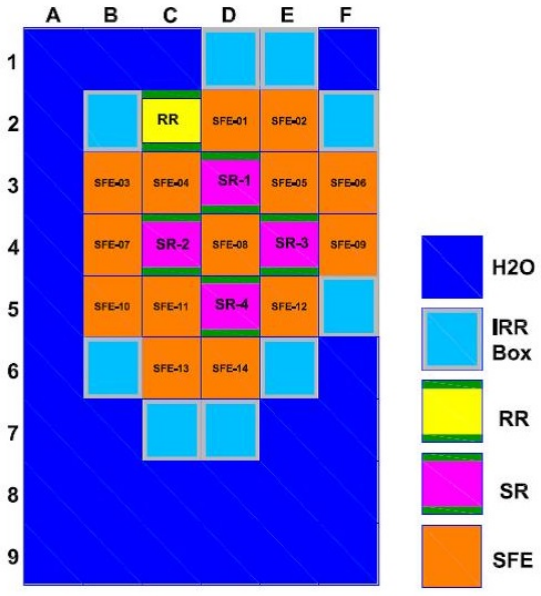

Figure 3: The arrangement of fresh fuel loading in "Core01".

Table 1: Main characteristics of TRR.

Parameters	Values
Fuel elements:	
U-235 per Standard Fuel Element (SFE)	290 g
U-235 per Control Fuel Element (CFE)	214 g
U per fuel plate	76 g
Meat:	
Enriched U_3O_8	20% in weight of U-235
U density	2.9617 g.cm^{-3}
Meat density	4.76 g.cm^{-3}
Void fraction	10.0%
Weight percentage	U-235 12.45%, U-238 49.78%, O 11.18%
Aluminum Meat	Purity 99.6% Density= 2.7 g.cm^{-3}
Frame and covers	Aluminum 6061 Density= 2.7 g.cm^{-3}
Shim and safety rods absorber	Ag-In-Cd Alloy (80, 15, 5% in weight respectively) Density= 10.17 g.cm^{-3}
Control rods' Cladding Material	AISI-316/L stainless steel Density= 7.95 g.cm^{-3}
Gap between absorber and clad	He (1 atm. pressure)
Regulating rod	AISI-316/L stainless steel Density= 7.95 g.cm^{-3}
Gird plate	Grid array X-Y Pitch: 7.71-8.1 cm
Grid plate material Grid z thickness Grid passing holes	AL-1100, 12.7 cm, 54 holes diameter: 6.19 cm Max, 6.17 cm Min 40 holes diameter: 2.222 With a reduction to 1.9053 cm
Reflectors	Water/Graphite

There are some basic assumptions for doing the mentioned calculations:

- The temperature of the fuel, fuel cladding, and the moderator or the coolant is assumed constant during the burn-up calculation.
- All control rods are withdrawal.
- The reactor thermal power is 5 MW.

To make the paper to be self-standing, in the following subsections, a brief description of the applied codes that have been used in the current investigation is described.

3.1 WIMS and CITATION Code

Cell calculation is performed by using the available versions of WIMSD: WIMSD5B. This code allows the user to select the collision probability method (using a selection of PERSEUS option in the input file) or discrete ordinate (Sn) transport solution method (using a selection of DSN option in the input file). The collision probability is usually recommended for small unit cells because of shorter running times and better flux solution quality. For large unit cells (that converging using PERSEUS is tricky) the DSN method is suggested. In the present work, 69 groups WIMS-D5 library format based on the IAEA WIMS Library Update Project (WLUP) is used. Table 2 shows the used neutron energy group structure for the library.

Table 2: The used group boundaries in the cell calculation.

Group number	Energy boundaries
1 (Fast)	10 MeV ∼ 5.53 keV
2 (Epi-Thermal)	5.53 keV ∼ 0.625 eV
3 (Thermal)	0.625 eV ∼ 0.0 eV

The WIMS code detailed description can be found in (Halsall, 1982) and (Stammler and Abbate, 1983). The burnup calculation in WIMS-D5 can be activated using POWERC card. The value of POWERC for the TRR case comes out to be 195.80 MW.te^{-1}. The depletion computations are executed in chains 12 and 16.

The CITATION code is used to predict the effective multiplication factor and isotopic concentration change during the burnup process. It solves the multi-group diffusion equation in 3D (Fowler et al., 1999). In our case (TRR with 5 MW thermal power), burnup calculation with a power of 5 MW continues until the reactivity reaches 1.8 (%). The considered EOC excess reactivity is intended to account for control reserve, experimental loads, and for change the CZP to HZP states (IAEA, 1992).

3.2 ORIGEN code

In the Oak Ridge Isotope GENeration (ORIGEN) code, burnup calculations are done by the solution of the Bateman equations using matrix exponential method (Croff, 1980a,b, 1983; Ludwig, 1999). It can calculate three groups of nuclides (720 activation products, 130 actinides, and 850 fission products). The ORIGEN2.1 uses Bateman equation as below:

$$\begin{aligned}\frac{\mathrm{d}N_i}{\mathrm{d}t} = &\sum_j \left[\gamma_{ji}\sigma_{f,j}N_j\varphi + \lambda_{ji}N_{ji}\right] + \sigma_{c,i-1}N_{i-1}\varphi \\ &- \sigma_{f,i}N_i\varphi - \sigma_{c,i}N_i\varphi - \lambda_i N_i\end{aligned} \quad (1)$$

where $i = 1, 2, .., I$, $\sum_j \gamma_{ji}\sigma_{f,j}N_j\varphi$ is yield rate of N_i due to fission of all nuclides N_j, $\sigma_{c,i-1}N_{i-1}\varphi$ is rate of trans-

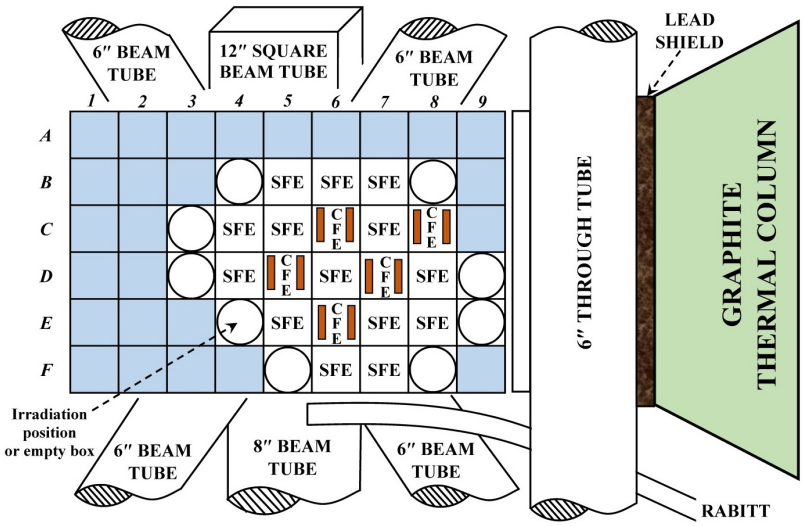

Figure 4: TRR first operating core configuration (IAEA, 2009).

mutation of N_{i-1} into N_i due to radioactive neutron capture, $\lambda_{ji}N_{ji}$ is the rate of formation of N_i due to the radioactive decay of N_j, $\sigma_{f,i}N_i\varphi$ is destruction rate of N_i due to fission, $\sigma_{c,i}N_i\varphi$ is destruction rate of N_i due to all forms of neutron absorption other than fission ((n,γ), (n,α), (n,p), $(n,2n)$, $(n,3n)$), and $\lambda_i N_i$ is loss due to radioactive decay of N_i.

ORIGEN2 assumes a homogenous medium with flux weighted average cross-section which is already should be provided for this code. Equation (1) is a coupled set of linear, homogenous, first-order differential equations with constant coefficients which can be written as below:

$$\dot{N} = A.N \tag{2}$$

where N is a vector of nuclide concentration and A is the matrix of transition. The transition matrix includes the rate of coefficients for decay and neutron absorption. The known solution based on the Matrix Exponential Method (MEM) is:

$$N = \exp(At).N(0) \tag{3}$$

where $N(0)$ is initial nuclide concentrations. The $\exp(At)$ can be expanded by:

$$\exp(At) = I + At + \frac{(At)^2}{2} + ... = \sum_{n=0}^{\infty} \frac{(At)^n}{n!} \tag{4}$$

where I is the unit matrix. However, producing the correct values of the matrix exponential function is difficult. The time-dependent solution can be written in terms of the rate constants a_{ij} from the transition matrix A as

$$\begin{aligned} N_i(t) = N_i(0) &+ t\sum_j a_{ij}N_j(0) \\ &+ \frac{t}{2}\sum_k \left[a_{ik}t\sum_j a_{kj}N_j(0)\right] \\ &+ \frac{t}{3}\sum_m \left\{a_{im}\frac{t}{2}\sum_k \left[a_{mk}t\sum_j a_{kj}N_j(0)\right]\right\} + ... \end{aligned} \tag{5}$$

Based on the techniques applied by Ball and Adams (Ball and Adams, 1967), ORIGEN usually separates the nuclides with a high rate of constants and treats them specially.

3.3 MCNPX

Monte Carlo N-Particle eXtended (MCNPX) code is a well-known, high precision, time-dependent code that can be used for almost all particles such as neutron, photon, electron. It is developed by Los Alamos National Laboratory. The energy range of the MCNPX is limited to that of 10^{-11} to 20 MeV. We used version 2.6 of MCNPX that includes 3-dimensional depletion and burnup capability. The MCNPX code uses CINDER90 deterministic code to perform the nuclide production and depletion part of the calculation. It uses a predictor-corrector calculation and a 63-group energy structure (ORIGEN code uses a weighted one-group structure). The CINDER90 can handle the time-dependent reactions of almost 3400 nuclides (Hendricks et al., 2008; Cuvelier, 2012; Fensin, 2008). The "cinder.dat" file of the CINDER90 code contains the required data for burn-up calculations.

4 Results of safety parameter analysis

This part describes various parameters that affect the safety of the reactor operation and at the same time can show the accuracy level of the simulated TRR using WIMS-CITATION. In other words, to determine if the model was constructed correctly in WIMS-CITATION, a comparison was made with SAR of TRR (IAEA, 2009). Table 3 presents the reactivity of TRR at cold zero state and hot zero states at different control rod positions of the first operating core configuration which is shown in Fig. 4. Besides, the results of the WIMS-CITATION code's have been compared with the previous work (Khoshahval and Davari, 2016).

Table 3: Reactivity of the "Core01" without thermal column and beam tube. The data reported as "Others' work" are related to (Khoshahval and Davari, 2016).

Core State	Shim-Safety Rods Percentage of Extraction C-4	D-3	E-4	D-5	Fine Rod Extraction (%)	Reactivity Calculated (pcm)	Reactivity SAR (pcm)	Reactivity (Others' work)	Δ (SAR) (%)	Δ (Others' work) (%)
CZP	100	100	100	100	100	6840	6934	6603	-1.35	3.59
CZP	100	100	100	100	0	6497	6364	6280	2.10	3.46
CZP	0	0	0	0	100	-11460	-12541	-14784	-8.62	-22.48
CZP	100	0	0	0	100	-5613	-6009	-7686	-6.59	-26.97
CZP	0	100	0	0	100	-5793	-6279	NA	-7.74	-
CZP	0	0	100	0	100	-6835	-7451	NA	-8.27	-
CZP	0	0	0	100	100	-6938	-7580	NA	-8.47	-
CZP	0	100	0	100	100	-2241	-2505	NA	-10.53	-
CZP	0	100	0	100	0	-2729	-3249	NA	-16.00	-
CZP	100	0	100	0	100	-2084	-2335	NA	-10.75	-
CZP	100	0	100	0	0	-2484	-2956	NA	-15.97	-
CZP	0	0	100	100	100	-2300	-2630	NA	-12.53	-
CZP	0	0	100	100	0	-2608	-3095	NA	-15.72	-
HZP	100	100	100	100	100	6688	6549	6414	2.12	4.27
HFP	100	100	100	100	100	3505	3319	3338	5.60	5.00

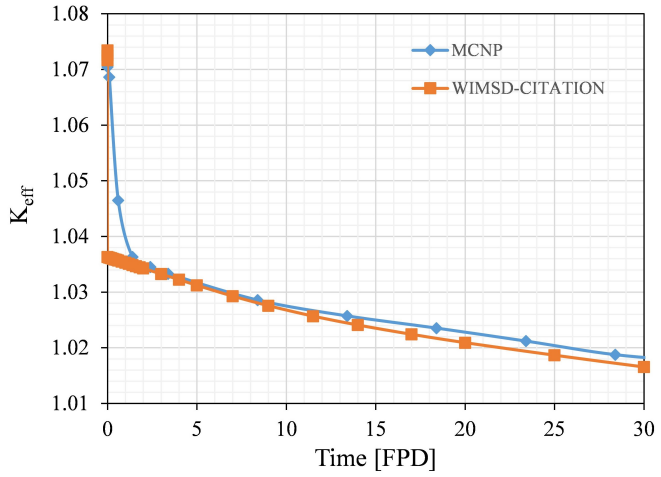

Figure 5: The Keff change versus time of the "Core01".

$$^{238}U + n \rightarrow {}^{239}U \xrightarrow{\beta^-} {}^{239}Np \xrightarrow{\beta^-} {}^{239}Pu$$

Figure 6: Neutron absorption in U-238.

Burn-up computations were also carried out by MCNPX using 500,000 neutron histories. Figure 5 illustrated the time evolution of the TRR multiplication factor determined by MCNPX and WIMS-CITATION codes. A good agreement is observed between WIMS-CITATION and the MCNPX. The large drop during the first burnup steps is due to the buildup of burnable poisons such as Xe-135 and depletion of the fresh fuel.

5 Isotopes inventory calculation

Each nuclide of the fuel changes as the burnup progresses. At the end of each operating cycle, the burned fuels include so many fission products, in addition to the remaining quantity of fissile material such a U-235 and 239Pu. Investigation of the amount of actinide and transuranic elements (TRU), Neptunium, Plutonium, Americium, and Curium are so important since TRU inventory is the main source of long-term heat generation in the spent fuels. Also, the performance of the high-level nuclear waste repository is dependent on TRU concentrations and compositions. However, TRU inventory is a valuable fuel resource (Kim et al., 2005; Westlén, 2007).

It is well known that during the reactor operation the concentration of the fuels continuously changes as nuclei of the fuels are transmuted by neutron absorption and subsequent decay (Ames II, 2010). Moreover, the buildup of fission products in the nuclear fuel that includes neutron-absorbing nuclides decreases the efficiency in the operation of the reactor. TRR fuel, U_3O_8AL is enriched in U-235 (20%) and the remaining uranium is made up of U-238 (80%). The constitutions of the TRU in the TRR are continuously varying and are dependent on initial enrichment, the level of neutron flux, burnup and TRR operation parameters. Figures 6 and 7 illustrate the essential actinides and their relations. The four of the most essential isotopes as indicated in Fig. 7 are Neptunium (Np), Americium (Am), Plutonium (Pu) and Curium (Cm).

Transmutation-decay in Fig. 7 indicates, Np-237 and Np-239 are generated by the beta-decay of U-237 and U-239, and subsequently, neutron capture in Np-237 and Np-239 results in Np-238 and Np-240 production. The Np-237 has one of the longest half-lives ($T_{1/2} = 2.14E6$ year), indicating it can be assumed a stable nuclide. The Am radioisotopes have different isotopes from Am-232 to Am-247. The Am-243 is an isotope with long half-life ($T_{1/2} = 7,370$ years), followed by the isotope (Am-241) with a half-life of 432.2 years. The Am-241 is produced from the Pu-241 decay ($T_{1/2} = 14.35$ years).

Pu radioisotopes (especially Pu-239 as a nuclear weapon component) are the most famous and prominent

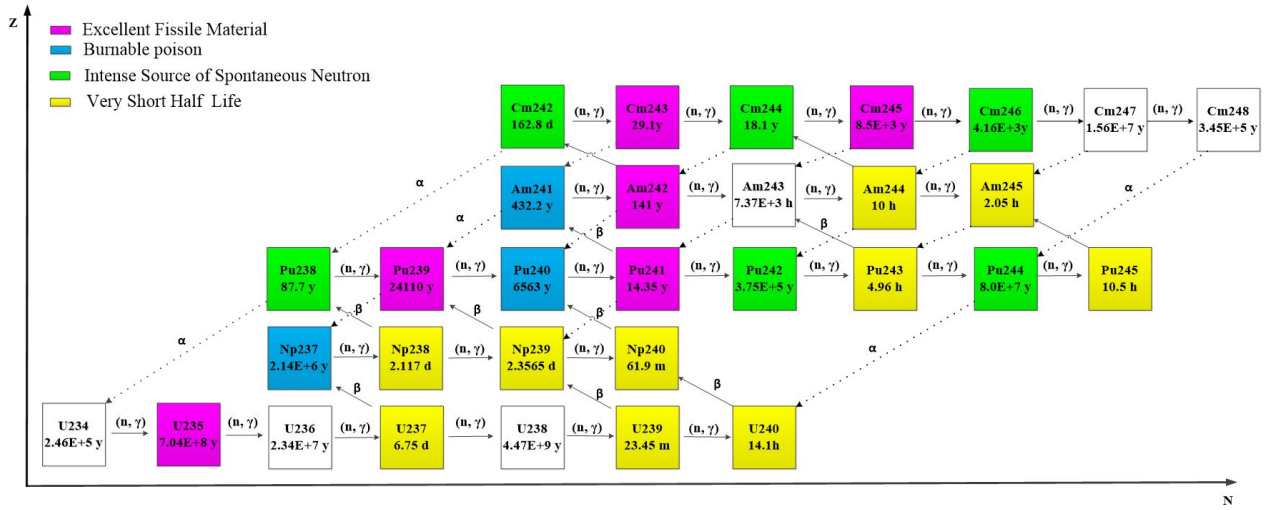

Figure 7: Scheme of transmutation and decay for important isotopes.

Table 4: Isotopic compositions of uranium and plutonium in SFE-08 (g).

Nuclide	Burnup, 0.0 (%), 0.0 (FPD)			Burnup, 1.8 (%), 11.5 (FPD)		
	WIMS-D5 & CITATION	ORIGEN	Differences (%)	WIMS-D5 & CITATION	ORIGEN	Differences (%)
U-235	2.9090E+02	2.9090E+02	0.00	2.8565E+02	2.8570E+02	-0.02
Pu-238	0.0000E+00	0.0000E+00	0.00	3.2516E-06	2.1790E-06	49.22
Pu-239	0.0000E+00	0.0000E+00	0.00	3.1823E-01	2.3060E-01	38.00
Pu-240	0.0000E+00	0.0000E+00	0.00	2.4089E-03	2.2580E-03	6.68
Pu-241	0.0000E+00	0.0000E+00	0.00	4.1687E-05	3.9830E-05	4.66
Pu-242	0.0000E+00	0.0000E+00	0.00	1.3142E-07	-	-
Nuclide	Burnup, 3.14 (%), 20 (FPD)			Burnup, 4.64 (%), 30 (FPD)		
	WIMS-D5 & CITATION	ORIGEN	Differences (%)	WIMS-D5 & CITATION	ORIGEN	Differences (%)
U-235	2.8183E+02	2.8190E+02	-0.02	2.7734E+02	2.7740E+02	-0.02
Pu-238	1.6381E-05	1.4590E-05	12.28	5.3646E-05	5.6140E-05	-4.44
Pu-239	6.1229E-01	4.6060E-01	32.93	9.4942E-01	7.2620E-01	30.74
Pu-240	7.9449E-03	7.8380E-03	1.36	1.8445E-02	1.8730E-02	-1.52
Pu-241	2.4053E-04	2.4700E-04	-2.62	8.4475E-04	9.0450E-04	-6.61
Pu-242	1.3225E-06	-	-	7.1111E-06	-	-

nuclides among TRUs. Pu-244 has a very long half-life ($T_{1/2} = 80$ million years). The Cm radioisotopes as alpha particle sources have been used as an X-ray spectrometer and as a fuel for radioisotope thermoelectric generators. The Cm has low concentrations in the spent fuel and their short half-lives greatly decrease the concern related to the high-level waste management

5.1 Inventory calculations of the first operating core of TRR

As said before, the discharge burnup changes the minor actinide content in the used fuel assemblies. It is known that high burnup fuels include americium, curium, and neptunium (DOE, 2002; Duderstadt and Hamilton, 1976). The "Core01" burnup distribution at 30 FPD is shown in Fig. 8. As can be seen in Fig. 8, assembly number 11 or SFE-08 (see Fig. 3) has the highest burnup among all of the fuel assemblies in the Core01. Table 4 shows the isotopic compositions of uranium and plutonium of the SFE-08.

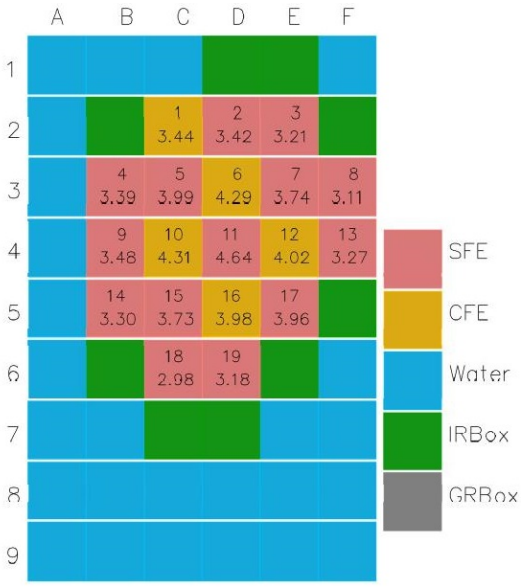

Figure 8: The "Core01" burnup distribution at 30th FPD (first line in is assembly number and the second line is denoted the burnup in %).

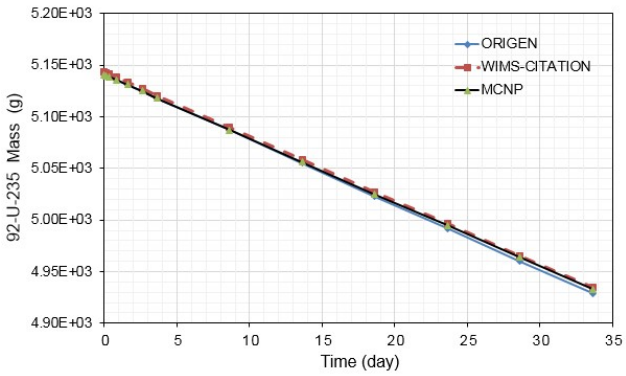

Figure 9: Mass of total U-235 as a function of time in Core01.

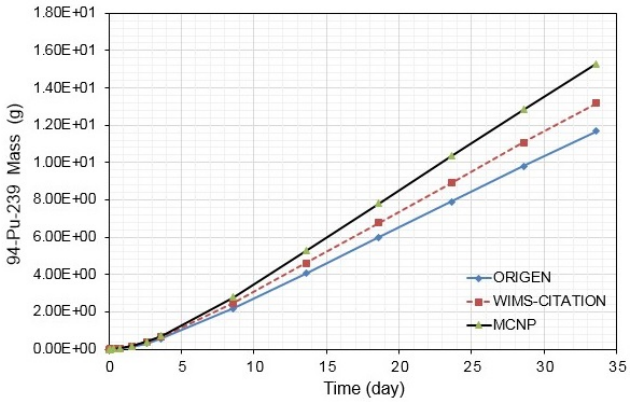

Figure 10: The total Pu-239 production in core01 versus time.

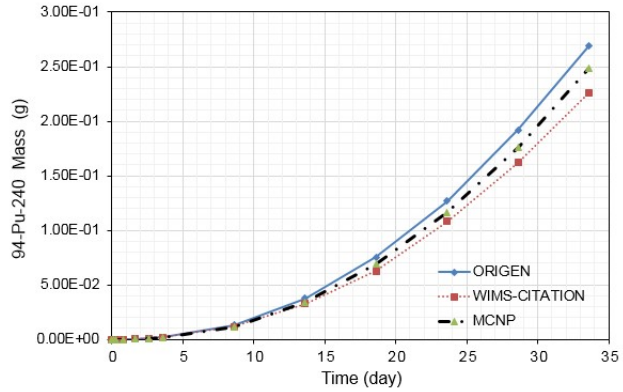

Figure 11: The total Pu-240 production in core01 versus time.

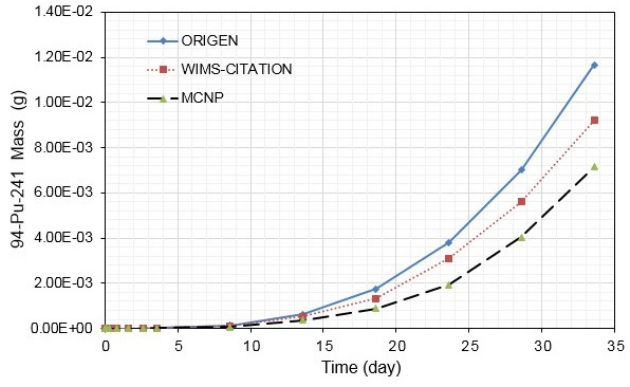

Figure 12: The total Pu-241 production in core01 versus time.

The variation of U-235 (fissile component of the fuel) mass with burn-up is depicted in Fig. 9. The U-235 depletion evaluations are in excellent agreement for three sets of codes (see Fig. 9). With burn-up time, the U-235 is decreased (depleted) linearly. As can be seen in Fig. 9 discrepancies of the U-235 concentration attained using ORIGEN, WIMS-CITATION and MCNPX are very small.

Figures 10, 11, and 12 show the production of Pu-239, Pu-240, and Pu-241 during fuel burnup. The production of Pu isotopes is due to neutron capturing by U-238. In addition, as can be seen in Fig. 10, the ORIGEN model is producing Pu-239 at a slower rate than the WIMS-CITATION model and MCNPX. There is a small difference in the quantities of Pu-240 and Pu-241 produced in three sets of used models (See Figs. 11 and 12). The Pu-240 and Pu-241 production are slightly greater in the ORIGEN model than the WIMS-CITATION model.

Figure 13 shows the rate of the variation of the higher actinides in the core. As can be seen in Fig. 13 the Pu-239 is the highest generated TRU nuclide in the fuel assembly. The values shown in Fig. 13 have resulted from WIMS-CITATION.

Table 5 illustrates the essential isotopes activities within the fuel assembly number 11 (SFE-08) at 30 FPD. As can be seen in Table 5, the agreement between the WIMS-CITATION and ORIGEN results is good for most of the cases but the maximum difference between the results for Rh-105, Np-237, ^{m}Te-127, Cs-134, I-135, ^{m}Pm-148, Pm-148, Pm-149, Np-237, Pu-239, Am-241, Am-242 is more than 20%. Figure 14 also shows the ratio of the calculated quantities of WIMS-CITATION to that of ORIGEN. In many of the actinides, the plot (Fig. 14) shows that the greater quantity produced using ORIGEN than in the WIMS-CITATION model. The calculated activity using WIMS-CITATION for Pu-239, ^{m}Pm-148, Cs-137, Cs-134, and ^{m}Te-127 is higher than those calculated by ORIGEN.

5.2 Inventory calculations of the 83th operating core of TRR

The composition of the fuel for the core configuration number 83 is also considered in this paper. This is the current core configuration of the TRR (See Figs. 15 and 16).

5.2.1 Isotope activity in the "Core83"

Depletion computations for core configuration number 83 were only done by WIMS-CITATION. Figure 17 shows the reactivity rundown of the TRR cycle 83. The initial reactivity of the core is 7705 pcm. It is worth mentioning that absorber control elements are assumed to be out of core.

Table 5: Activity of important isotopes available in SFE-08 (Ci) at 30 FPD.

Nuclide	WIMSD-CITATION	ORIGEN	Difference (%)	Nuclide Nuclide	WIMSD-CITATION	ORIGEN	Difference (%)
Ru-103	3.53130E+03	3.88300E+03	-9.1	U-235	5.99640E-04	5.99900E-04	0.0
Ru-106	6.97710E+01	7.30400E+01	-4.5	U-236	1.46200E-04	1.59900E-04	-8.6
Ru-105	2.26200E+03	2.83600E+03	-20.2	U-238	3.90470E-04	3.90800E-04	-0.1
Sb-125	2.15460E+00	2.26500E+00	-4.9	Np-237	4.29460E-06	5.71400E-06	-24.8
^{m}Te-127	1.31680E+01	9.92400E+00	32.7	Np-239	2.27650E+04	2.34800E+04	-3.0
Cs-134	2.11170E+00	1.53500E+00	37.6	Pu-238	9.17840E-04	9.61400E-04	-4.5
Cs-137	3.63010E+01	3.44300E+01	5.4	Pu-239	5.88780E-02	4.51600E-02	30.4
I-135	1.48480E+04	1.85800E+04	-20.1	Pu-240	4.18770E-03	4.27000E-03	-1.9
Xe-135	3.93920E+03	3.99100E+03	-1.3	Pu-241	8.74700E-02	9.32200E-02	-6.2
Pm-147	6.69640E+01	7.74100E+01	-13.5	Am-241	3.88390E-06	2.85700E-06	35.9
Pm-148m	1.61270E+01	9.83300E+00	64.0	Am-242	9.50420E-04	1.89100E-03	-49.7
Pm-148	8.27450E+01	1.09600E+02	-24.5	^{m}Am-242	2.16070E-08	-	-
Pm-149	2.58430E+03	3.23200E+03	-20.0	Cm-242	3.25900E-05	3.61400E-05	-9.8
Sm-151	5.54000E-01	5.74800E-01	-3.6	Cm-243	2.50110E-10	-	-
Eu-155	9.27730E-01	1.09900E+00	-15.6	Cm-244	1.12210E-08	-	-

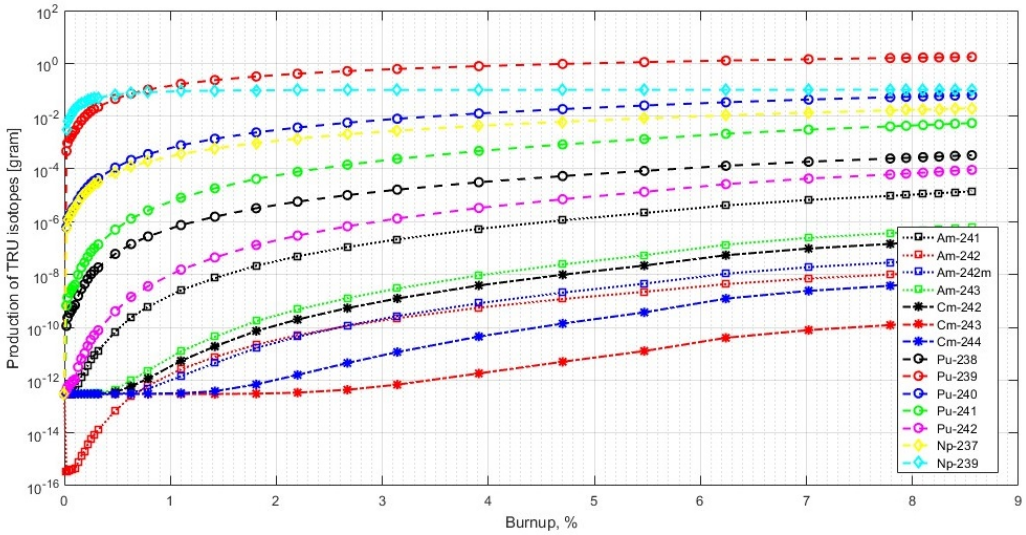

Figure 13: The resulting fuel compositions (isotopic vector) for the TRU of TRR in SFE-08.

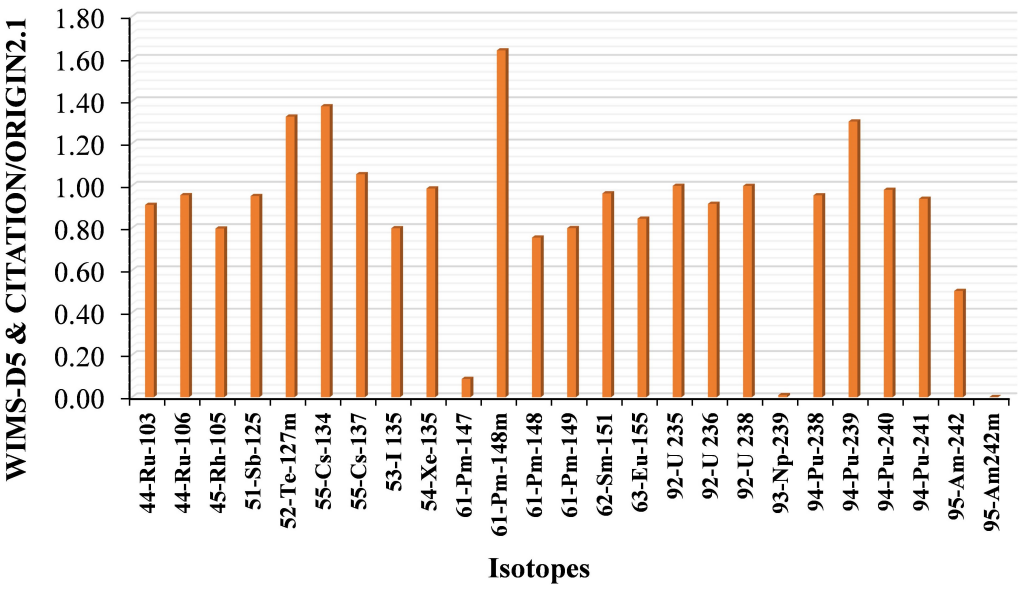

Figure 14: The "Core01" relative activities at 30 FPD.

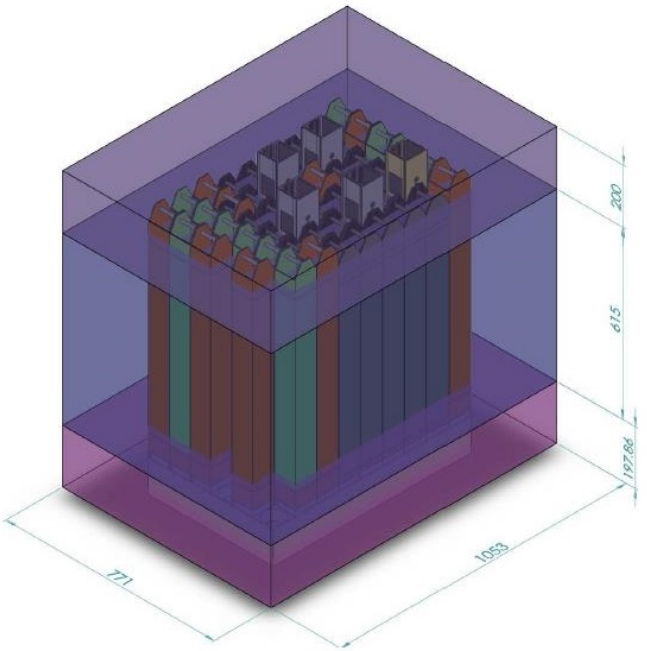

Figure 15: The schematic of "Core83" model of TRR Reactor in CITATION code.

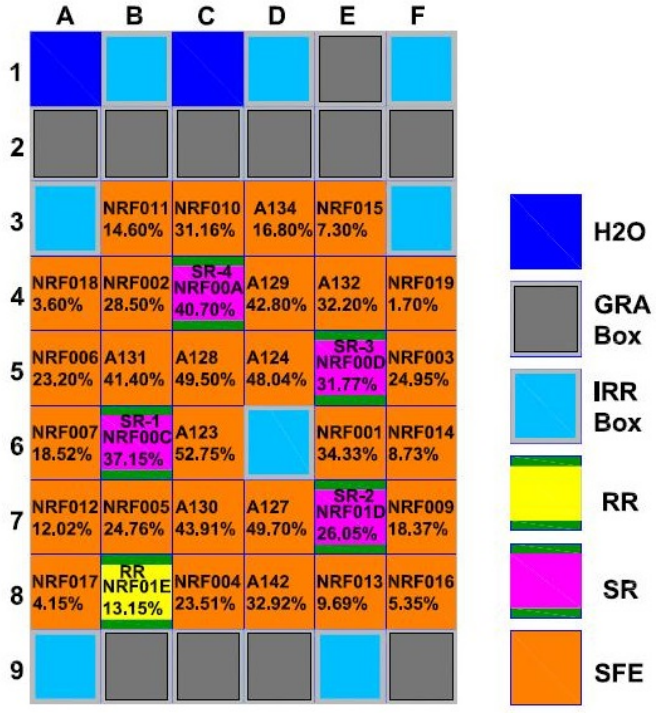

Figure 16: The arrangement of burnup fuel loading in "Core83".

The activity (Ci) of the important isotopes available in "Core83" are given in three-time steps (0.0, 30, and 55 FPD) of burnup calculations respectively (Tables 6, 7, and 8). As can be seen in Table 8, fuel after 55 FPD contains 94.2% plutonium, 0.1% americium, 0.01% Cm and 5.67% of neptunium. Therefore, the plutonium that is a direct creation from neutron capture in U-238, is the most dominating presence among all transuranic and curium has the lowest production over the lifetime and at EOC. Finally, the total radioactivity of the TRR core at the end of cycle 83 is calculated by summing the radio activities of all the radionuclides at the end of the core life and it is evaluated to be 6.47×10^5 Ci. In addition, the normalized values for actinide inventory for the first and 83^{th} operating cycles can be seen graphically in Fig. 18.

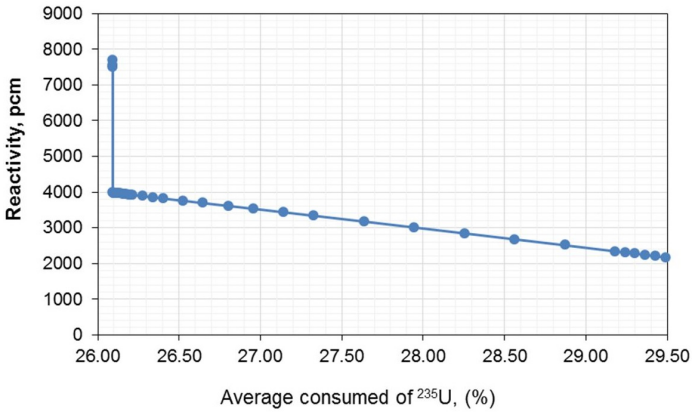

Figure 17: The "Core83" excess reactivity versus average consumed U-235.

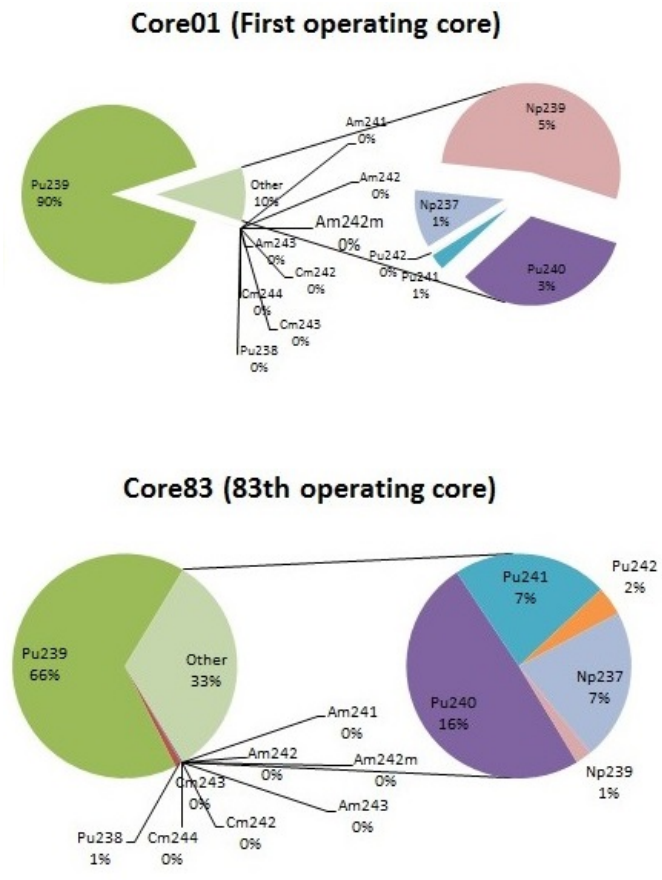

Figure 18: Normalized weight percentage of the transuranic present in a TRR fuel assembly.

Table 6: The mass and activity of isotopes available in "Core83", at 0.0 (FPD).

Burnup, 26.09 (%)								
Nuclide	Mass (g)	Activity (Ci)	Nuclide	Mass (g)	Activity (Ci)	Nuclide	Mass (g)	Activity (Ci)
O-nat	8.2753E+03	0.0000E+00	Cd-113	8.9335E-03	3.5145E-05	Eu-152	1.1792E-03	2.0507E-01
Al-nat	1.9681E+04	0.0000E+00	In-115	1.0405E-01	7.3547E-14	Eu-153	3.2060E+00	0.0000E+00
Gd-154	1.2217E-02	0.0000E+00	Sb-125	3.3548E-01	3.4789E+02	Eu-154	2.9323E-01	7.9308E+01
Gd-155	1.2773E-03	0.0000E+00	^{m}Te-127	7.0400E-02	6.8250E+02	Eu-155	1.9917E-01	9.6694E+01
Gd-156	2.6335E-01	0.0000E+00	I-127	1.6648E+00	0.0000E+00	U-234	1.7694E-03	1.1077E-05
Gd-157	1.3983E-03	0.0000E+00	Xe-131	3.0975E+01	0.0000E+00	U-235	6.8451E+03	1.4800E-02
Gd-158	1.7329E-01	0.0000E+00	Cs-133	7.5008E+01	0.0000E+00	U-236	3.8495E+02	2.4896E-02
Dy-160	2.3637E-06	0.0000E+00	Cs-134	1.9683E+00	2.5434E+03	U-237	2.0516E-08	0.0000E+00
Dy-161	2.4903E-03	0.0000E+00	Cs-137	7.4324E+01	6.4538E+03	U-237	2.7276E-01	0.0000E+00
Dy-162	1.4003E-03	0.0000E+00	I-135	7.7842E-02	2.7466E+05	U-238	3.6633E+04	1.2313E-02
Dy-163	6.0540E-04	0.0000E+00	Xe-134	9.1152E+01	4.1965E-18	Np-237	6.6445E+00	4.6710E-03
Dy-164	1.2978E-04	0.0000E+00	Xe-135	3.5423E-02	9.0039E+04	Np-239	1.9414E+00	4.4912E+05
Ho-165	1.6124E-04	0.0000E+00	Cs-135	2.5696E+01	2.9599E-02	Pu-238	5.4808E-01	9.3772E+00
Er-166	7.2517E-06	0.0000E+00	Xe-136	1.2388E+02	9.0205E-16	Pu-239	1.2519E+02	7.7636E+00
Er-167	5.3846E-08	0.0000E+00	Nd-143	6.5761E+01	0.0000E+00	Pu-240	1.6925E+01	3.8426E+00
Kr-83	3.5653E+00	0.0000E+00	Nd-145	4.8053E+01	0.0000E+00	Pu-241	5.5532E+00	5.7500E+02
Mo-95	5.2924E+01	0.0000E+00	Pm-147	9.7369E+00	9.0303E+02	Pu-242	6.1921E-01	2.4412E-03
Tc-99	5.1644E+01	8.8365E-01	Sm-147	3.9030E+00	8.9468E-08	Am-241	1.0507E-01	3.5894E-01
Ru-101	4.5252E+01	0.0000E+00	^{m}Pm-148	1.2822E-01	2.7394E+03	Am-242	8.5150E-05	6.8780E+01
Ru-103	4.0129E+00	1.2977E+05	Pm-148	5.7419E-02	9.4383E+03	^{m}Am-242	9.2488E-04	9.6868E-03
Ru-106	3.1832E+00	1.0563E+04	Sm-148	2.6760E+00	9.2353E-13	Am-243	2.1911E-02	4.3836E-03
Rh-103	2.1725E+01	0.0000E+00	Pm-149	1.3409E-01	5.3185E+04	Cm-242	8.0717E-03	2.6681E+01
Rh-105	5.7427E-02	4.8628E+04	Sm-149	3.9381E-01	0.0000E+00	Cm-243	4.3677E-05	2.2083E-03
Pd-105	9.4815E+00	0.0000E+00	Sm-150	1.4067E+01	0.0000E+00	Cm-244	1.3995E-03	1.1329E-01
Pd-107	2.1870E+00	1.1258E-03	Sm-151	1.0205E+00	2.6862E+01	FP4902*	1.0583E+03	0.0000E+00
Pd-108	1.0548E+00	0.0000E+00	Sm-152	7.4657E+00	0.0000E+00	-	-	-
Ag-109	6.2002E-01	0.0000E+00	Eu-151	1.5908E-03	2.2186E-18	-	-	-

*Lumped fission product

Table 7: The mass and activity of isotopes available in "Core83", at 30.0 (FPD).

Burnup, 27.95 (%)								
Nuclide	Mass (g)	Activity (Ci)	Nuclide	Mass (g)	Activity (Ci)	Nuclide	Mass (g)	Activity (Ci)
O-nat	8.2753E+03	0.0000E+00	Cd-113	8.9983E-03	3.5400E-05	Eu-152	1.2296E-03	2.1384E-01
Al-nat	1.9681E+04	0.0000E+00	In-115	1.1140E-01	7.8742E-14	Eu-153	3.5203E+00	0.0000E+00
Gd-154	1.4318E-02	0.0000E+00	Sb-125	3.6066E-01	3.7400E+02	Eu-154	3.3038E-01	8.9353E+01
Gd-155	1.3611E-03	0.0000E+00	^{m}Te-127	7.2737E-02	7.0515E+02	Eu-155	2.1580E-01	1.0477E+02
Gd-156	2.8727E-01	0.0000E+00	I-127	1.8027E+00	0.0000E+00	U-234	2.1558E-03	1.3496E-05
Gd-157	1.3985E-03	0.0000E+00	Xe-131	3.3349E+01	0.0000E+00	U-235	6.6582E+03	1.4395E-02
Gd-158	1.8941E-01	0.0000E+00	Cs-133	8.0903E+01	0.0000E+00	U-236	4.1474E+02	2.6823E-02
Dy-160	2.6354E-06	0.0000E+00	Cs-134	2.2155E+00	2.8628E+03	U-237	2.0674E-08	0.0000E+00
Dy-161	2.7328E-03	0.0000E+00	Cs-137	8.0239E+01	6.9674E+03	U-237	2.9402E-01	0.0000E+00
Dy-162	1.5735E-03	0.0000E+00	I-135	7.7821E-02	2.7459E+05	U-238	3.6615E+04	1.2307E-02
Dy-163	6.8604E-04	0.0000E+00	Xe-134	9.8465E+01	4.5332E-18	Np-237	7.4324E+00	5.2249E-03
Dy-164	1.4377E-04	0.0000E+00	Xe-135	3.4799E-02	8.8452E+04	Np-239	1.9662E+00	4.5485E+05
Ho-165	1.8487E-04	0.0000E+00	Cs-135	2.7595E+01	3.1787E-02	Pu-238	6.4332E-01	1.1007E+01
Er-166	8.1386E-06	0.0000E+00	Xe-136	1.3402E+02	9.7587E-16	Pu-239	1.3306E+02	8.2518E+00
Er-167	6.2712E-08	0.0000E+00	Nd-143	7.0559E+01	0.0000E+00	Pu-240	1.8733E+01	4.2531E+00
Kr-83	3.8345E+00	0.0000E+00	Nd-145	5.1823E+01	0.0000E+00	Pu-241	6.3260E+00	6.5503E+02
Mo-95	5.7121E+01	0.0000E+00	Pm-147	1.0369E+01	9.6161E+02	Pu-242	7.5100E-01	2.9608E-03
Tc-99	5.5724E+01	9.5346E-01	Sm-147	4.3450E+00	9.9599E-08	Am-241	1.2379E-01	4.2290E-01
Ru-101	4.8877E+01	0.0000E+00	^{m}Pm-148	1.3714E-01	2.9299E+03	Am-242	1.0212E-04	8.2490E+01
Ru-103	4.1374E+00	1.3380E+05	Pm-148	6.1959E-02	1.0185E+04	^{m}Am-242	1.1051E-03	1.1574E-02
Ru-106	3.4203E+00	1.1350E+04	Sm-148	3.0187E+00	1.0418E-12	Am-243	2.7876E-02	5.5771E-03
Rh-103	2.3556E+01	0.0000E+00	Pm-149	1.3541E-01	5.3708E+04	Cm-242	9.9501E-03	3.2890E+01
Rh-105	5.8091E-02	4.9190E+04	Sm-149	3.9097E-01	0.0000E+00	Cm-243	5.6670E-05	2.8653E-03
Pd-105	1.0285E+01	0.0000E+00	Sm-150	1.5258E+01	0.0000E+00	Cm-244	1.8753E-03	1.5181E-01
Pd-107	2.4000E+00	1.2355E-03	Sm-151	1.0497E+00	2.7631E+01	FP4902*	1.1429E+03	0.0000E+00
Pd-108	1.1656E+00	0.0000E+00	Sm-152	8.0834E+00	0.0000E+00	-	-	-
Ag-109	6.8445E-01	0.0000E+00	Eu-151	1.6470E-03	2.2970E-18	-	-	-

*Lumped fission product

Table 8: The mass and activity of isotopes available in "Core83", at 55.0 (FPD).

Burnup, 29.49 (%)								
Nuclide	Mass (g)	Activity (Ci)	Nuclide	Mass (g)	Activity (Ci)	Nuclide	Mass (g)	Activity (Ci)
O-nat	8.2753E+03	0.0000E+00	Cd-113	8.9693E-03	3.5286E-05	Eu-152	1.2687E-03	2.2063E-01
Al-nat	1.9681E+04	0.0000E+00	In-115	1.1736E-01	8.2958E-14	Eu-153	3.7909E+00	0.0000E+00
Gd-154	1.6262E-02	0.0000E+00	Sb-125	3.8137E-01	3.9548E+02	Eu-154	3.6341E-01	9.8289E+01
Gd-155	1.4262E-03	0.0000E+00	^{m}Te-127	7.4147E-02	7.1882E+02	Eu-155	2.2978E-01	1.1155E+02
Gd-156	3.0769E-01	0.0000E+00	I-127	1.9182E+00	0.0000E+00	U-234	2.5270E-03	1.5819E-05
Gd-157	1.3972E-03	0.0000E+00	Xe-131	3.5308E+01	0.0000E+00	U-235	6.5030E+03	1.4060E-02
Gd-158	2.0320E-01	0.0000E+00	Cs-133	8.5792E+01	0.0000E+00	U-236	4.3938E+02	2.8417E-02
Dy-160	2.8746E-06	0.0000E+00	Cs-134	2.4357E+00	3.1474E+03	U-237	2.0810E-08	0.0000E+00
Dy-161	2.9414E-03	0.0000E+00	Cs-137	8.5159E+01	7.3946E+03	U-237	3.1184E-01	0.0000E+00
Dy-162	1.7280E-03	0.0000E+00	I-135	7.7798E-02	2.7451E+05	U-238	3.6600E+04	1.2302E-02
Dy-163	7.5887E-04	0.0000E+00	Xe-134	1.0456E+02	4.8137E-18	Np-237	8.1283E+00	5.7141E-03
Dy-164	1.5601E-04	0.0000E+00	Xe-135	3.4269E-02	8.7107E+04	Np-239	1.9876E+00	4.5982E+05
Ho-165	2.0651E-04	0.0000E+00	Cs-135	2.9152E+01	3.3579E-02	Pu-238	7.3186E-01	1.2521E+01
Er-166	8.9266E-06	0.0000E+00	Xe-136	1.4249E+02	1.0376E-15	Pu-239	1.3925E+02	8.6355E+00
Er-167	7.0892E-08	0.0000E+00	Nd-143	7.4474E+01	0.0000E+00	Pu-240	2.0305E+01	4.6100E+00
Kr-83	4.0559E+00	0.0000E+00	Nd-145	5.4949E+01	0.0000E+00	Pu-241	7.0156E+00	7.2643E+02
Mo-95	6.0608E+01	0.0000E+00	Pm-147	1.0872E+01	1.0083E+03	Pu-242	8.7702E-01	3.4576E-03
Tc-99	5.9112E+01	1.0114E+00	Sm-147	4.7316E+00	1.0846E-07	Am-241	1.4099E-01	4.8165E-01
Ru-101	5.1895E+01	0.0000E+00	^{m}Pm-148	1.4433E-01	3.0835E+03	Am-242	1.1812E-04	9.5411E+01
Ru-103	4.2080E+00	1.3608E+05	Pm-148	6.5726E-02	1.0804E+04	^{m}Am-242	1.2720E-03	1.3323E-02
Ru-106	3.6155E+00	1.1998E+04	Sm-148	3.3246E+00	1.1474E-12	Am-243	3.3854E-02	6.7731E-03
Rh-103	2.5096E+01	0.0000E+00	Pm-149	1.3653E-01	5.4152E+04	Cm-242	1.1763E-02	3.8883E+01
Rh-105	5.8645E-02	4.9660E+04	Sm-149	3.8630E-01	0.0000E+00	Cm-243	6.9873E-05	3.5329E-03
Pd-105	1.0961E+01	0.0000E+00	Sm-150	1.6255E+01	0.0000E+00	Cm-244	2.3775E-03	1.9247E-01
Pd-107	2.5838E+00	1.3301E-03	Sm-151	1.0653E+00	2.8040E+01	FP4902*	1.2134E+03	0.0000E+00
Pd-108	1.2624E+00	0.0000E+00	Sm-152	8.6016E+00	0.0000E+00	-	-	-
Ag-109	7.4053E-01	0.0000E+00	Eu-151	1.6849E-03	2.3499E-18	-	-	-

*Lumped fission product

Table 9: Mass of isotopes available in fuel assembly "A123", at 55.0 (FPD).

Burnup, 29.49 (%)								
Nuclide	Mass (g)	Activity (Ci)	Nuclide	Mass (g)	Activity (Ci)	Nuclide	Mass (g)	Activity (Ci)
O-nat	2.6118E+02	0.0000E+00	Cd-113	2.4266E-04	9.5464E-07	Eu-151	4.1087E-05	5.7301E-20
Al-nat	6.2115E+02	0.0000E+00	In-115	6.4117E-03	4.5323E-15	Eu-152	3.6355E-05	6.3225E-03
Gd-154	2.0877E-03	0.0000E+00	Sb-125	2.2283E-02	2.3108E+01	Eu-153	2.8679E-01	0.0000E+00
Gd-155	7.4305E-05	0.0000E+00	^{m}Te-127	2.3331E-03	2.2618E+01	Eu-154	3.4753E-02	9.3994E+00
Gd-156	2.1878E-02	0.0000E+00	I-127	1.2288E-01	0.0000E+00	Eu-155	1.6004E-02	7.7697E+00
Gd-157	4.2388E-05	0.0000E+00	Xe-131	2.0888E+00	0.0000E+00	U-234	4.1628E-04	2.6060E-06
Gd-158	1.4831E-02	0.0000E+00	Cs-133	5.2060E+00	0.0000E+00	U-235	1.2587E+02	2.7214E-04
Dy-160	2.6169E-07	0.0000E+00	Cs-134	2.3293E-01	3.0099E+02	U-236	2.6283E+01	1.6999E-03
Dy-161	2.2766E-04	0.0000E+00	Cs-137	5.2409E+00	4.5508E+02	U-237	7.5577E-10	0.0000E+00
Dy-162	1.6864E-04	0.0000E+00	I-135	2.4487E-03	8.6401E+03	U-237	1.9968E-02	0.0000E+00
Dy-163	8.0263E-05	0.0000E+00	Xe-134	6.4853E+00	2.9858E-19	U-238	1.1458E+03	3.8512E-04
Dy-164	1.3429E-05	0.0000E+00	Xe-135	7.9123E-04	2.0111E+03	Np-237	7.5150E-01	5.2830E-04
Ho-165	2.3957E-05	0.0000E+00	Cs-135	1.6709E+00	1.9247E-03	Np-239	7.9864E-02	1.8476E+04
Er-166	8.6604E-07	0.0000E+00	Xe-136	9.0123E+00	6.5624E-17	Pu-238	9.8269E-02	1.6813E+00
Er-167	9.1662E-09	0.0000E+00	Nd-143	4.1846E+00	0.0000E+00	Pu-239	6.9706E+00	4.3228E-01
Kr-83	2.3598E-01	0.0000E+00	Nd-145	3.3283E+00	0.0000E+00	Pu-240	1.7012E+00	3.8625E-01
Mo-95	3.7116E+00	0.0000E+00	Pm-147	5.4527E-01	5.0569E+01	Pu-241	7.6973E-01	7.9702E+01
Tc-99	3.6074E+00	6.1725E-02	Pm-147	6.1489E-01	5.7026E+01	Pu-242	1.4387E-01	5.6719E-04
Ru-101	3.2145E+00	0.0000E+00	Sm-147	3.9775E-01	9.1174E-09	Am-241	1.9591E-02	6.6925E-02
Ru-103	1.4469E-01	4.6792E+03	^{m}Pm-148	7.4908E-03	1.6003E+02	Am-242	1.8315E-05	1.4794E+01
Ru-106	2.1415E-01	7.1066E+02	Pm-148	4.0052E-03	6.5835E+02	^{m}Am-242	1.9202E-04	2.0112E-03
Rh-103	1.5764E+00	0.0000E+00	Sm-148	3.2095E-01	1.1077E-13	Am-243	6.8909E-03	1.3786E-03
Rh-105	2.1893E-03	1.8538E+03	Pm-149	4.9460E-03	1.9618E+03	Cm-242	2.0883E-03	6.9028E+00
Pd-105	7.2291E-01	0.0000E+00	Sm-149	9.3900E-03	0.0000E+00	Cm-243	1.5235E-05	7.7028E-04
Pd-107	1.9926E-01	1.0258E-04	Sm-150	1.0423E+00	0.0000E+00	Cm-244	5.7823E-04	4.6810E-02

5.2.2 Isotope activity in highest burned up fuel assembly in the "Core83"

The isotopes activity and the mass of the fuel assembly (A123 (C-6) in Fig. 16) with the highest burn-up are presented in Table 9 at 55 FPD. Lastly, the total radioactivity of the FA-A123 of TRR core has been computed, summing the radio activities of all the radionuclides at the end of the core life and were evaluated to be 2.19×10^4 Ci.

6 Conclusions

Fuel isotopes inventory evaluations of Tehran Research Reactor is analyzed in this study. TRU of TRR inventory is responsible for long-term heat generation and radiotoxicity. In addition, the comparison and verification study was performed in this investigation with WIMS-CITATION, ORIGEN, and MCNPX codes. It is shown that the 94% of the TRU produced during the TRR operation is Pu. Moreover, the agreement of the results attained with the three mentioned methods is quite good for most of the evaluated isotopes. However, as indicated, in some cases the results are terrible. Indeed, some of the actinides (such as Cs-134, Rh-105, ^{m}Te-127, I-135, ^{m}Pm-148, Pm-148, Pm-149, Np-237, Pu-239, Am-241, and Am-242) have a significant difference. The reason for such difference came from different nuclear data used by the applied methods and possibly model difference as well. The results demonstrate that the WIMS-CITATION model produces slightly more Pu-239 than the ORIGEN model. Moreover, the total radioactivity of the TRR core at the end of the reactor core operation is estimated to be 6.47×10^5 Ci.

Conflict of Interest

The authors declare no potential conflict of interest regarding the publication of this work.

References

Al Zain, J., El Hajjaji, O., and El Bardouni, T. (2018). Calculation of the activity inventory for the MNSR reactor using DRAGON4 code. *Radiation Physics and Chemistry*, 151:179–185.

Ames II, D. E. (2010). *High-fidelity nuclear energy system optimization towards an environmentally benign, sustainable, and secure energy source*. Texas A&M University.

Ball, S. and Adams, R. (1967). MATEXP, A general purpose digital computer program for solving ordinary differential equations by the matrix exponential method. Technical report, Oak Ridge National Lab., Tenn.

Croff, A. (1980a). ORIGEN 2.1. Isotope Generation and Depletion Code. *ORNL/TM-7175, July*.

Croff, A. (1980b). ORIGEN2: a revised and updated version of the oak ridge isotope generation and depletion code. Technical report, Oak Ridge National Lab., TN (USA).

Croff, A. G. (1983). ORIGEN2: a versatile computer code for calculating the nuclide compositions and characteristics of nuclear materials. *Nuclear Technology*, 62(3):335–352.

Cuvelier, M.-H. (2012). *Advanced Fuel Cycle Scenarios with AP1000 PWRs and VHTRs and Fission Spectrum Uncertainties*. PhD thesis, Texas A & M University.

DOE, U. (2002). Environmental Impact Statement for a Geologic Repository for the Disposal of Spent Nuclear Fuel and High-Level Radioactive Waste at Yucca Mountain, Nye County, Nevada.

Duderstadt, J. J. and Hamilton, L. J. (1976). *Nuclear reactor analysis*. Wiley.

Fensin, M. L. (2008). *Development of the MCNPX depletion capability: A Monte Carlo linked depletion method that automates the coupling between MCNPX and CINDER90 for high fidelity burnup calculations*. University of Florida.

Fowler, T., Vondy, D., and Cunningham, G. (1999). CITATION-LDI2 nuclear reactor core analysis code system. *CCC-643, Oak Ridge National Laboratory, Oak Ridge, Tennessee*.

Halsall, M. (1982). LWR-WIMS, a computer code for light water reactor lattice calculations. Technical report, UKAEA Atomic Energy Establishment.

Hassan, H. H., Ghazi, N., and Hainoun, A. (2008). Analysis of MNSR core composition changes using the codes WIMSD-4 and CITATION. *Applied Radiation and Isotopes*, 66(10):1492–1500.

Hendricks, J. S., McKinney, G. W., Fensin, M. L., et al. (2008). MCNPX 2.6. 0 Extensions. *Los Alamos National Laboratory*, page 73.

IAEA (1992). IAEA-TECDOC-643, Research reactor core conversion guidebook, Volume 2: Analysis (Appendices A-F). Technical report, International Atomic Energy Agency.

IAEA (2009). Final Safety Analysis Report of the Tehran Research Reactor. Technical report, International Atomic Energy Agency.

Khattab, K. (2005). Calculations of fuel burn-up and radionuclide inventory in the syrian miniature neutron source reactor using the WIMSD4 code. *Annals of Nuclear Energy*, 32(10):1122–1130.

Khoshahval, F. and Davari, A. (2016). Safety requirement assessment of fuel sample test in Tehran research reactor. *Progress in Nuclear Energy*, 91:208–216.

Kim, T., Taiwo, T., Hill, R., et al. (2005). A feasibility study of reactor-based deep-burn concepts. Technical report, Argonne National Lab.(ANL), Argonne, IL (United States).

Ludwig, S. (1999). ORIGEN2, Version 2.1 (August 1, 1991) Release Notes. *Oak Ridge National Laboratory, revised May*.

Stammler, R. J. and Abbate, M. J. (1983). Methods of steady-state reactor physics in nuclear design.

Westlén, D. (2007). *Why Faster is Better: On Minor Actinide Transmutation in Hard Neutron*. PhD thesis, KTH.

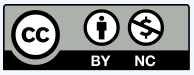

To cite this article:

Khoshahval, F., Rajaee, M., Tehrani, N. (2023). Isotopic discharge concentrations of Tehran research reactor using deterministic and Monte Carlo methods. *Radiation Physics and Engineering*, 4(1), 39-51.

DOI: 10.22034/rpe.2022.347567.1092

To link to this article: https://doi.org/10.22034/rpe.2022.347567.1092